



## Numerical studies on heat transfer and friction factor characteristics of a tube fitted with helical screw-tape without core-rod inserts

Xiaoyu Zhang, Zhichun Liu, Wei Liu\*

School of Energy and Power Engineering, Huazhong University of Science and Technology, Wuhan 430074, China

### ARTICLE INFO

#### Article history:

Received 6 January 2012

Received in revised form 21 May 2012

Accepted 15 January 2013

Available online 9 February 2013

#### Keywords:

Helical screw-tape

Numerical simulation

Core-flow

Heat transfer enhancement

Physical quantity synergy analysis

Entropy generation minimization

### ABSTRACT

The principle of heat transfer enhancement in the core flow of tube has been proposed to improve the temperature uniformity and reduce flow resistance, which is different from that of heat transfer enhancement in the boundary flow of tube. Helical screw-tape inserts with four different widths ( $w = 7.5$  mm, 12 mm, 15 mm and 20 mm) have been investigated for different inlet volume-flow rates ranging from 200 L/h to 500 L/h. A three-dimensional turbulence analysis of heat transfer and fluid flow is performed by numerical simulation. The simulation results show that the average overall heat transfer coefficients in circular plain tubes are enhanced with helical screw-tape of different widths by as much as 212 ~ 351% at a constant tube-side temperature and the friction factor are enhanced by as much as 33% to 1020%. The PEC value of the helical screw-tape inserts of different width varies between 1.58 and 2.35. Physical quantity synergy analysis is performed to investigate the mechanism of heat transfer enhancement. The synergy angles  $\alpha$ ,  $\beta$ ,  $\gamma$ ,  $\theta$  and  $\eta$  are calculated, and the numerical results verify the synergy regulation among physical quantities of fluid particle in the flow field of convective heat transfer, which can guide the optimum design for better heat transfer units and high-efficiency heat exchangers. Entropy generation analysis is also performed to explain how to get the optimum helical screw-tape.

© 2013 Elsevier Ltd. All rights reserved.

### 1. Introduction

Heat exchangers, which are widely used in many fields such as power generation, chemical industry, metallurgy, steel production, refrigeration, air-conditioning etc., are indispensable general devices for heat transfer. The most significant variables in reducing the size and cost of a heat exchanger are heat transfer coefficient and pressure drop or flow resistance. An increase in the heat transfer coefficient often leads to an increase in the flow resistance, thereby reducing energy efficiency. The main challenge for heat exchangers design is to minimize the flow resistance while enhancing the heat transfer coefficients.

Generally speaking, tube flow can be divided into two parts [1]: boundary flow and core flow. The methods of surface-based heat transfer enhancement are the common methods to enhance heat transfer in the tube. While these measures are effective for heat transfer, however, viscous resistance of fluid initiated from the wall surface would lead to significant increase in flow resistance, which is a cost for more efficient heat convection. To overcome this inherent weakness of surface-based enhancement, a number of experiments have been conducted on fluid-based enhancement [2–4]. In theory, Liu and Yang have proposed four

principles for increasing efficiency for core flow [5]. The first two principles have to do with enhancing the uniformity of core flow temperature by increasing the effective thermal conductivity of the fluid and disturbing the fluid of the core flow field. The third principle suggests that velocity gradient inside tube should be minimized to reduce fluid shear force. Finally, the continuous extended surface should be broken to avoid large surface friction so that the disturbance to the boundary may be reduced to avoid large momentum loss [6]. Nevertheless, few studies have been conducted to verify the four principles. This study intends to fill the gap by simulating the heat transfer and flow resistance in a tube fitted with helical screw-tape without core-rod inserts.

In the past work, the twisted-tape inserts are extensively used in the heat transfer enhancement of many heat exchangers. Manglik and Bergles [2,3] reported the experimental data for twisted-tape and presented predictive correlations for laminar and turbulent flows under uniform wall temperature condition. Saha and Gaitonde [7] used the regularly spaced twisted tape elements connected by thin circular rods to investigate heat transfer enhancement in a circular tube. Date and Gaitonde [8] introduced the correlations for predicting characteristics of laminar flow in a tube fitted with regularly spaced twisted tape elements. Ventsislav [9] presented the enhancement of heat transfer by a combination of a single start spirally corrugated tubes with twisted tapes in turbulent flow and presented empirical correlation along with

\* Corresponding author. Tel.: +86 02787542618.

E-mail address: [w\\_liu@mail.hust.edu.cn](mailto:w_liu@mail.hust.edu.cn) (W. Liu).

## Nomenclature

$Be$	Bejan number	$s$	pitch of helical screw-tape (m)
$c_p$	the specific heat at constant pressure (kJ/kg K)	$T$	temperature (K)
$d_1$	inner diameter of helical screw-tape (m)	$u$	the flow velocity (m/s)
$d_2$	outer diameter of helical screw-tape (m)	$\nu_t$	kinematic eddy viscosity ( $\text{m}^2 \text{s}^{-1}$ )
$D$	the tube diameter (m)	Greek symbols	
$f$	friction factor	$\alpha$	synergy angle ( $^\circ$ )
$h$	the average heat transfer coefficient in the tube ( $\text{W}/\text{m}^2 \text{K}$ )	$\beta$	synergy angle ( $^\circ$ )
$k$	turbulent kinetic energy ( $\text{m}^2/\text{s}^2$ )	$\gamma$	synergy angle ( $^\circ$ )
$L$	the length of tube (m)	$\theta$	synergy angle ( $^\circ$ )
$Nu$	average Nusselt number	$\eta$	synergy angle ( $^\circ$ )
$(N_s)_T$	entropy generation number from heat transfer irreversibility	$\rho$	density of water ( $\text{kg}/\text{m}^3$ )
$(N_s)_P$	entropy generation number from fluid friction irreversibility	$\delta$	Kronecker delta
$N_s$	entropy generation number	$\lambda$	thermal conductivity ( $\text{W}/\text{m K}$ )
$\dot{m}$	mass flow rate in tube per unit tape length ( $\text{kg}/\text{m s}$ )	$\tau$	shear stress (Pa)
$P$	pressure ( $\text{N}/\text{m}^2$ )	$\omega$	specific turbulence dissipation rate ( $\text{s}^{-1}$ )
$q'$	heat transfer rate per unit tape length ( $\text{W}/\text{m}$ )	Subscripts	
$Re$	Reynolds number	0	plain tube
$\dot{S}'_{gen}$	the entropy generation rate per unit tape length ( $\text{W}/\text{m K}$ )	$m$	mean
		$w$	wall

performance prediction. Chang et al. [10] experimentally studied the axial heat transfer distribution and friction factor for the tubes fitted with broken twisted tapes of different twisted ratios, and found that local Nusselt number and mean friction factor increased with the decrease of twisted ratio. Naphon [11] compared tubes with twisted inserts with those without twisted-tape inserts, and proposed non-isothermal correlations for predicting the heat transfer coefficient and friction factor of the horizontal pipe with twisted-tape inserts.

Helical screw-tape is a modified form of a twisted tape wound on a single rod. Both the helical screw-tape and the twisted-tape generate a similar swirling flow in the circular tube, but they exhibit different characteristics of flow. For the helical screw-tape, the swirling flow rotates in single way smooth direction of flow like a screw motion, while the twisted-tape generates the swirling flow in two way directions of parallel flows simultaneously (two parallel flows separated by the twisted-tape). Sivashanmugam and Suresh [12–15] studied the heat transfer and friction factor characteristics of the laminar and turbulent flows in a circular tube fitted with full-length helical screw-tapes with different twist ratios, including the increasing and decreasing order of twist ratio sets. Eiamsa-ard and Promvong [16] reported enhancement of heat transfer in a tube with regularly-spaced helical tape swirl generator with Reynolds number between 2300 and 8800 using water as working fluid, and concluded that the full-length helical tape with rod provides the highest heat transfer rate about 10% better than that without rod. Ibrahim [17] experimentally investigated the heat transfer characteristics and friction factor in the horizontal double pipes of flat tubes with full length helical screw element of different twist ratio and helical screw inserts with different spacer length and found that the Nusselt number and friction factor decreased with the increase of spacer length for flat tube. Guo et al. [18] numerically studied the circular tube fitted with helical screw-tape inserts from the viewpoint of field synergy principle, they compared the results based on the RNG k-epsilon turbulence model with those based on the SST k-omega turbulence model, and concluded that the SST k-omega turbulence model performs much better than k-epsilon turbulence model both qualitatively and quantitatively, in terms of agreement with the experiment. Eiamsa-ard and Promvong [4]

experimentally investigated the enhancement of heat transfer in a concentric double tube heat exchanger fitted with loose-fit, regularly spaced and full-length helical screw-tape swirl generators. Contrasting the tape with core-rod and that without core-rod, it was found that the heat transfer rate obtained without core-rod was higher than that with core-rod around 25%–60% while the friction resistance without core-rod was around 50% lower. Furthermore, the enhancement efficiency for the helical screw-tape without core-rod was about 2 times higher than that with the core-rod. Focusing on the helical screw-tape without core-rod but varying the tape widths, this paper numerically investigates the heat transfer and friction factor characteristics of turbulent flow through a circular tube helical screw-tape.

However, as mentioned above, there are extensive literatures investigating the tubes fitted with helical tape inserts, they mainly focused on the performance of heat transfer and flow resistance, the mechanism of heat transfer enhancement is rarely reported. So it is worthwhile studying the novel mechanism of heat transfer enhancement, which could serve as a guideline to optimize heat exchangers and design new-type heat transfer enhancement apparatus. Guo et al. [19,20] proposed the field synergy principle which indicates that the heat transfer rate depends not only on the velocity and temperature fields but also on their synergy which is related to an integral of the inner product of the temperature gradient and the velocity field. Liu et al. [21–23] developed Guo's field synergy principle and proposed that there exists other synergistic relation among physical quantities besides the velocity and temperature fields. Improving synergistic relation among physical quantities is beneficial to heat transfer enhancement. In the recent design work of a thermal system, the efficient utilization of energy has been treated as an essential consideration except the analysis from the view point of Thermodynamic First Law. Irreversibility and entropy generation in the flow field have been adopted as a gauge for evaluating the optimization of a thermal system. Based on the minimal entropy generation principle [24,25], considerable optimal designs of thermal systems have been proposed [26–31]. However, as for helical screw-tape, most of past researches were restricted to the Thermodynamic First Law. The relevant entropy generation analysis is still very rare.

In the present study, we attempt to explain the enhanced heat transfer mechanism of tubes fitted with helical screw-tape inserts from the viewpoint of field synergy principle and minimal entropy generation principle, and analyze novel helical screw-tape without core-rod based on these principles.

## 2. Methods

### 2.1. Physics and mathematic model

For the physical model shown in Fig. 1, the calculation parameters are obtained as follows: the tube length  $L = 1500$  mm, diameter  $D = 25$  mm, inner diameter of helical screw-tape  $d_1 = 5$  mm, outer diameter  $d_2 = 12.5$  mm, 17 mm, 20 mm, 25 mm, the tape thickness  $t = 1$  mm, pitch  $s = 18$  mm. The tape width  $W = d_2 - d_1$  has four values, 7.5 mm, 12 mm, 15 mm and 20 mm. In this study, the fluid is water, and inlet temperature is 353 K, wall temperature is taken as 298 K.

In order to obtain the mathematic model, the following assumptions are made: (1) The physical properties of fluid are constant; (2) fluid is incompressible, isotropic and continuous; (3) fluid is Newton fluid; (4) the effect of gravity is negligible.

In the turbulence modeling, the velocity vector  $\mathbf{u}$  is firstly decomposed into two parts, the mean velocity  $\bar{\mathbf{u}} = (u_1, u_2, u_3)^T$  and the fluctuation part  $u' = (u'_1, u'_2, u'_3)^T$ , that is,

$$\mathbf{u} = \bar{\mathbf{u}} + \mathbf{u}' \quad (1)$$

If the time average is applied, then we have

$$\bar{\mathbf{u}} = \frac{1}{\Delta t} \int_t^{t+\Delta t} \mathbf{u} dt \quad (2)$$

where  $\Delta t$  is time scale. The governing equation of time-averaged incompressible flows are written as follows [32]:

Continuity equation:

$$\frac{\partial(\rho \bar{u}_i)}{\partial x_i} = 0 \quad (3)$$

Momentum equation:

$$\frac{\partial(\rho \bar{u}_i)}{\partial t} + \frac{\partial(\rho \bar{u}_i \bar{u}_j)}{\partial x_j} = -\frac{\partial \bar{P}_i}{\partial x_i} + \frac{\partial}{\partial x_j} \left( \mu \frac{\partial \bar{u}_i}{\partial x_j} - \rho \bar{u}'_i \bar{u}'_j \right) \quad (4)$$

Energy equation:

$$\frac{\partial(\rho \bar{T})}{\partial x_i} + \frac{\partial(\rho \bar{u}_i \bar{T})}{\partial x_i} = \frac{\partial}{\partial x_i} \left( \frac{\lambda}{c_p} \frac{\partial \bar{T}}{\partial x_i} \right) \quad (5)$$

Turbulence kinetic energy:

$$\frac{D(\rho k)}{Dt} = \bar{\tau}_{ij} \frac{\partial \bar{u}_i}{\partial x_j} - \beta^* \rho \omega k + \frac{\partial}{\partial x_j} \left[ (\mu + \sigma_k \mu_t) \frac{\partial k}{\partial x_j} \right] \quad (6)$$

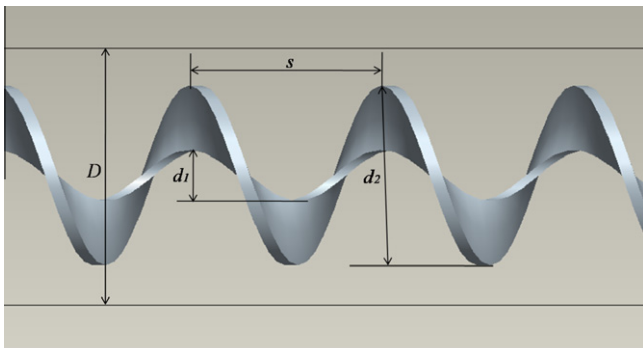


Fig. 1. The model of helical screw-tape.

Specific dissipation rate:

$$\frac{D(\rho \omega)}{Dt} = \frac{\gamma}{\nu_t} \bar{\tau}_{ij} \frac{\partial \bar{u}_i}{\partial x_j} - \beta^* \rho \omega^2 + \frac{\partial}{\partial x_j} \left[ (\mu + \sigma_\omega \mu_t) \frac{\partial \omega}{\partial x_j} \right] + 2\rho(1 - F_1) \sigma_{\omega 2} \frac{1}{\omega} \frac{\partial k}{\partial x_j} \frac{\partial \omega}{\partial x_j} \quad (7)$$

where the kinematic eddy viscosity is given by

$$\nu_t = \frac{\alpha_1 k}{\max(\alpha_1 \omega, SF_2)} \quad (8)$$

The shear stress is given by

$$\bar{\tau}_{ij} = \mu_t \left( \frac{\partial \bar{u}_i}{\partial x_j} + \frac{\partial \bar{u}_j}{\partial x_i} - \frac{2}{3} \frac{\partial \bar{u}_k}{\partial x_k} \delta_{ij} \right) - \frac{2}{3} \rho k \delta_{ij} \quad (9)$$

here,  $\delta_{ij}$  is the Kronecker delta. The strain rate tensor is given by

$$S_{ij} = \frac{1}{2} \left( \frac{\partial u_i}{\partial x_j} + \frac{\partial u_j}{\partial x_i} \right) \quad (10)$$

The other relations are listed as follows:

$$F_1 = \tan h \left\{ \left\{ \min \left[ \max \left( \frac{\sqrt{k}}{\beta^* \omega y}, \frac{500\nu}{y^2 \omega} \right), \frac{4\sigma_{\omega 2} k}{CD_{k\omega} y^2} \right] \right\}^4 \right\} \quad (11)$$

where,

$$CD_{k\omega} = \max \left( 2\rho \sigma_{\omega 2} \frac{1}{\omega} \frac{\partial k}{\partial x_j} \frac{\partial \omega}{\partial x_j}, 10^{-10} \right) \quad (12)$$

$$F_2 = \tan h \left\{ \left[ \max \left( \frac{2\sqrt{k}}{\beta^* \omega y}, \frac{500\nu}{y^2 \omega} \right) \right]^2 \right\} \quad (13)$$

$$\varphi = F_1 \varphi_1 + (1 - F_1) \varphi_2 \quad (14)$$

The constants for the SST  $k - \omega$  model are:  $\beta_1 = 0.075$ ,  $\beta_2 = 0.0828$ ,  $\beta^* = 0.09$ ,  $\sigma_{k1} = 0.85$ ,  $\sigma_{k2} = 1$ ,  $\sigma_{\omega 1} = 0.5$ ,  $\sigma_{\omega 2} = 0.856$ ,  $\gamma_1 = 0.5532$ ,  $\gamma_2 = 0.4404$ .

Eqs. (3)–(14) with the boundary conditions are solved by SIMPLE algorithm to demonstrate velocity, temperature and pressure fields. After computing velocity and temperature fields, heat transfer coefficient of tube flow can be calculated as

$$h = \frac{q}{T_w - T_m} \quad (15)$$

where  $T_m$  is fluid bulk temperature inside tube:

$$T_m = \frac{\int_0^R u T r dr}{\int_0^R u r dr} \quad (16)$$

Nusselt number and friction factor for a tube can be calculated as

$$Nu = \frac{hD}{\lambda} \quad (17)$$

$$f = \frac{2\Delta PD}{L\rho u_m^2} \quad (18)$$

where  $u_m$  is the mean velocity in the tube.

To evaluate the effect of heat transfer enhancement under given pumping power, the formula of performance evaluation criteria is employed as [33,34]

$$PEC = \frac{Nu/Nu_0}{(f/f_0)^{1/3}} \quad (19)$$

where  $Nu$  and  $Nu_0$  are Nusselt numbers for the enhanced tube and the smooth tube respectively,  $f$  and  $f_0$  are friction coefficients for enhanced tube and smooth tube respectively.

## 2.2. Numerical method

All the above-mentioned equations accompanied by boundary conditions are discretized using finite volume formulation. In the equations, the momentum terms, the turbulent kinetic energy terms, the turbulent dissipation rate terms and the temperature terms are modeled by the second-order upwind scheme. The numerical solution procedure adopts the well-known semi-implicit SIMPLE algorithm. The detailed numerical procedure can be found in the book of Patankar [35]. The convergent criterion is set as the relative residual of all variables, including mass, velocity components, temperature, turbulent kinetic energy and turbulent dissipation rate less than  $10^{-6}$ . A commercial CFD software Fluent is used for the numerical solutions.

## 3. Results and analysis

### 3.1. Grid independent tests

For validating the accuracy of numerical solutions, the grid independent tests have been performed by using three different grid systems with 552,801, 1310,343 and 2264,272 grids to calculate the flow field in tube. The test problem is the turbulent convection in a tube inserted with helical screw-tape of  $W = 12$  mm and inlet volume-flow rate is 450 L/h. From calculated values of Nusselt numbers obtained by the three grid systems, the 552,801-grid system is found to be dense enough to result in the grid independent solutions. Accordingly, the grid system with 552,801 grids is employed to perform the following calculations.

### 3.2. Heat transfer

Effects of the helical screw-tape without core-rod on the heat transfer are depicted in Fig. 2. And Fig. 3 shows the temperature contours of the tube fitted with the helical screw tape of different widths for  $Re = 10233$ . Fig. 4 shows the variation of  $Nu$  number along the length of the tube for  $Re = 10233$ . It is found that the tubes with helical screw-tape inserted all lead to higher heat transfer rates than that of the plain tube. This can be attributed to swirling effect created from the use of the helical screw-tape, making temperature more uniform in the core flow, therefore, causing higher temperature gradient in the radial direction. Furthermore, the swirl enhances the flow turbulence, leading to more efficient convection heat transfer. Thus, the higher the Reynolds number

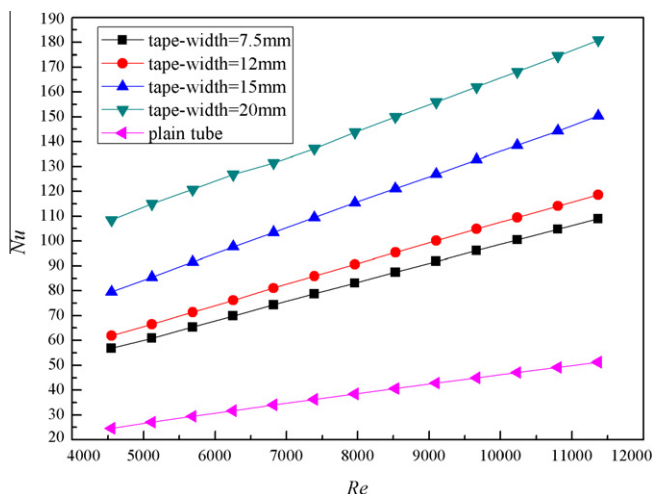


Fig. 2. Variation of Nusselt number with Reynolds number for helical tapes of different widths.

is, the greater the heat transfer rate would be. As shown in the Fig. 4, the  $Nu$  number is higher in the entrance area because of the thinner thermal boundary layer. Moreover, the wider the helical screw-tape is, the higher heat transfer rate would be. That is because the twist ratio of the helical screw-tape is increasing while the helical screw-tape is wider and the pitch length is constant. Therefore, the heat transfer surface area is larger and the area which has uniform temperature field is larger, thereby leading to higher temperature gradient.

### 3.3. Friction factor

Fig. 5 shows the variation of friction factors with Reynolds numbers for the helical screw-tape without core-rod inserted in the tube. And the pressure contours of the tube fitted with the helical screw tape of different widths for  $Re = 10233$  are depicted in Fig. 6. Fig. 7 shows the variation of friction factor along the length of the tube for  $Re = 10233$ . As expected, the friction factors obtained from the tube with the helical screw-tape are significantly higher than that from the plain tube. The friction factor changes little along the length of tube. And the wider the helical screw-tape is, the higher the friction factor would be. There are four reasons: (1) as the width of the helical screw-tape decreases, the flow disturbance in the tube has changed from the flow disturbance near the tube wall to the flow disturbance in the core flow. When the flow disturbs the fluid near the wall, the velocity gradient is very high near the tube wall, causing great flow resistance. While the flow disturbs the core flow, the velocity gradient is much lower and the flow resistance is much smaller correspondingly; (2) as the width of helical screw-tape is decreased, the surface area is smaller when the fluid flows through the helical screw-tape, thus, making the flow resistance lower; (3) the twist ratio of the helical screw-tape is decreasing while the pitch length is constant. The swirling effect is weakening, so that the flow resistance is decreasing; (4) for the width of the helical screw-tape equal to  $D - d_1 = 20$  mm, the fluid can only flow through the hollow core-rod, greatly lengthening the flow path, and thereby increasing the flow resistance.

### 3.4. The overall heat transfer performance

As shown in Fig. 8, the PEC values may reach 1.58 ~ 2.35 for helical screw-tape as  $Re$  number ranges in 4000 ~ 12000. The overall performance has improved greatly with helical screw-tape without core-rod inserts. In other words, heat transfer enhancement with helical screw-tape inserts in the core flow form an equivalent thermal boundary layer in the fully developed tube flow, which consequently enlarges the temperature gradient of the fluid near the tube wall, and thereby enhances the heat transfer between the fluid and the tube wall. At the same time, the increase of flow resistance in the tube is not so obvious. It is noteworthy that the helical screw-tape of  $W = 15$  mm has the highest PEC value among the four helical screw-tapes. While the width of the helical screw-tape equals to  $D - d_1 = 20$  mm, the PEC value is the lowest of the four for most  $Re$  numbers in the range.

## 4. Comparison with the past experiment

Eiamsa-ard and Promvong [4] experimentally investigated the enhancement of heat transfer in a concentric double tube heat exchanger fitted with loose-fit, regularly spaced and full-length helical screw-tape swirl generators. The model is the same as the helical screw-tape of 12 mm width and other conditions are the same as well. And the empirical correlations for Nusselt number, friction factor and PEC were proposed as follows:

$$Nu = 0.0215 Re^{0.9143} Pr^{1/3} \quad (20)$$

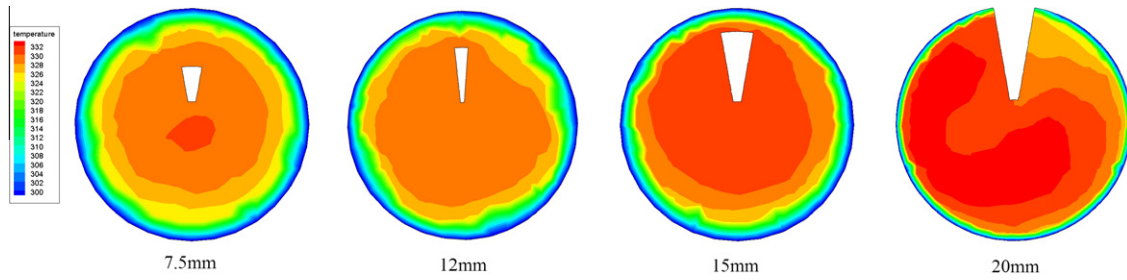


Fig. 3. The temperature contours of the tube fitted with the helical screw tape of different widths for  $Re = 10233$ .

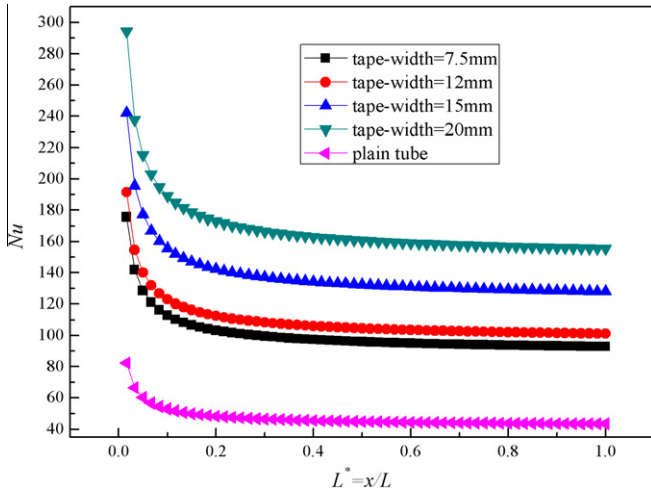


Fig. 4. Variation of  $Nu$  number along the length of the tube for  $Re = 10233$ .

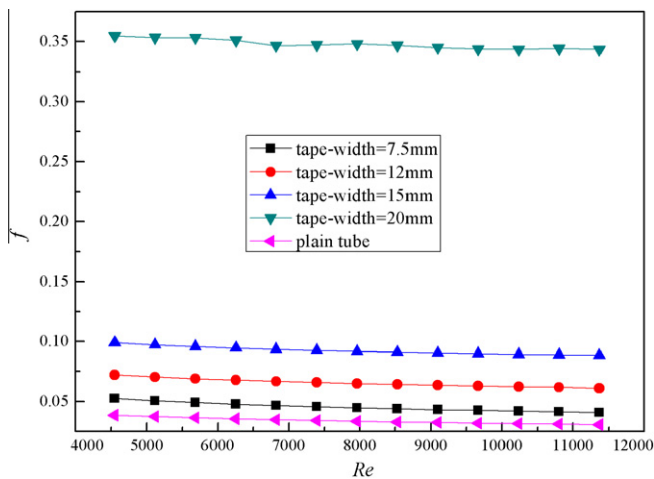


Fig. 5. Variation of friction factor with Reynolds number for helical tapes of different widths.

$$f = 8.098 Re^{-0.47} \quad (21)$$

$$PEC = 1.44 Re^{0.42} \quad (22)$$

As shown in Figs. 9–11, the simulated data are consistent with the experimental data on the whole, but they still have some differences on Nusselt Numbers, friction factors and PEC values. There are three reasons to explain the differences between experimental and simulated data: (1) the helical screw-tape has thermal conduction in the experiment while in the simulation we only consider

swirling effect of the helical screw-tape; (2) in the experiment there are inlet effects, bubbles factor and etc. making friction factor inaccurate, while in the simulation these factors are neglected; (3) the physical parameters that are variational in the experiment remain constant in the simulation.

### 5. Physical quantity synergy analysis

On the basis of the principle of field synergy for heat transfer enhancement [19,20], Liu et al. [21–23] set up the concept of physical quantity synergy in the laminar and turbulent flow field according to the physical mechanism of convective heat transfer between fluid and tube wall, which reveals the synergy regulation among physical quantities of fluid particles. The physical nature of enhancing heat transfer and reducing flow resistance, which is directly associated with synergy angles  $\alpha, \beta, \gamma, \theta, \eta$ , is also explained.

The synergy angles among velocity, velocity gradient and temperature gradient of a fluid particle  $M$  in the flow field can be written as

$$\alpha = \arccos \frac{\mathbf{U} \cdot \nabla u}{|\mathbf{U}| |\nabla u|} \quad (23)$$

$$\beta = \arccos \frac{\mathbf{U} \cdot \nabla T}{|\mathbf{U}| |\nabla T|} \quad (24)$$

According to vector relation of a fluid particle  $M$ , the synergy angle between temperature gradient  $\nabla T$  and velocity component gradient  $\nabla u$  can be expressed as

$$\gamma = \arccos \frac{\nabla T \cdot \nabla u}{|\nabla T| |\nabla u|} \quad (25)$$

The synergy angle between velocity  $\mathbf{U}$  and pressure gradient  $\nabla p$  can be expressed as

$$\theta = \arccos \frac{\mathbf{U} \cdot \nabla p}{|\mathbf{U}| |\nabla p|} \quad (26)$$

The synergy angle between temperature gradient  $\nabla T$  and pressure gradient  $\nabla p$  can be expressed as

$$\eta = \arccos \frac{\nabla T \cdot \nabla p}{|\nabla T| |\nabla p|} \quad (27)$$

Fig. 12 shows the effect of  $Re$  number on average synergy angle  $\alpha$  for helical screw-tape of different widths. As shown in the figure, average synergy angle  $\alpha$  between fluid velocity  $\mathbf{U}$  and velocity gradient  $\nabla u$  is decreased as the width of helical screw-tape increases, so it can be known that flow resistance of fluid will increase.

Fig. 13 shows the effect of  $Re$  number on average synergy angle  $\beta$  for helical screw-tape of different widths. As shown in the figure, average synergy angle  $\beta$  between fluid velocity  $\mathbf{U}$  and temperature gradient  $\nabla T$  is also decreased as the width of helical screw-tape increases. Therefore it can be known that heat transfer will be enhanced between the fluid and the tube wall.

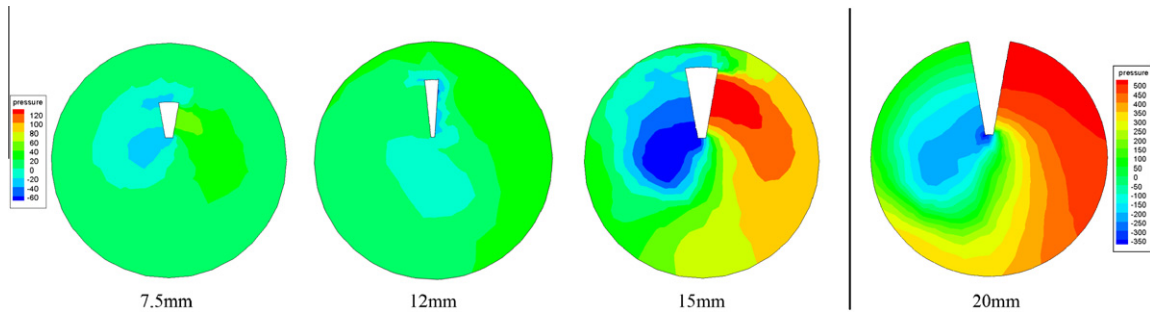


Fig. 6. The pressure contours of the tube fitted with the helical screw tape of different widths for  $Re = 10233$ .

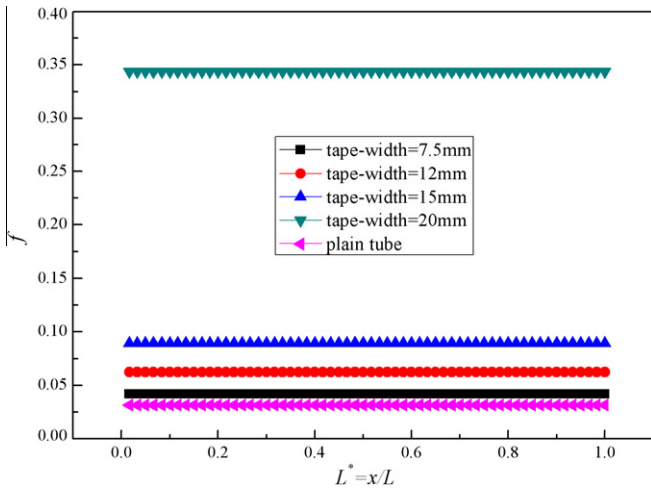


Fig. 7. Variation of friction factor along the length of the tube for  $Re = 10233$ .

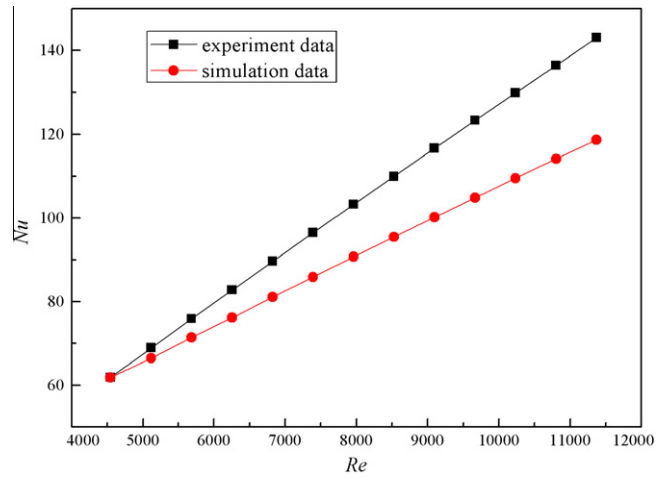


Fig. 9.  $Nu$  comparison between experimental data and simulated data.

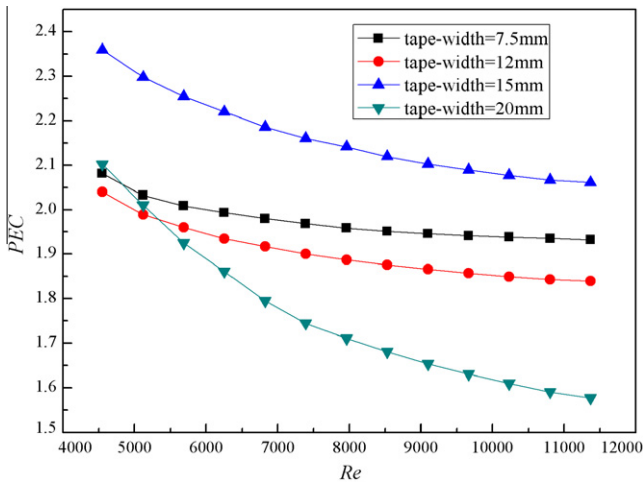


Fig. 8. The PEC value versus Reynolds number.

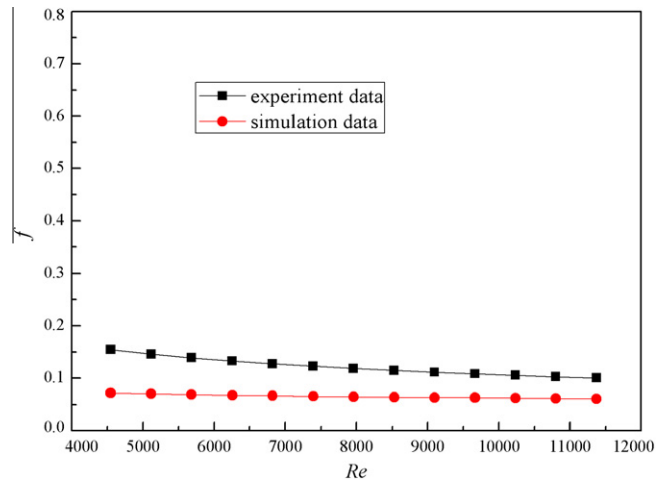


Fig. 10.  $f$  comparison between experimental data and simulated data.

Fig. 14 shows the variation of average synergy angle  $\gamma$  with  $Re$  for heat-transfer enhanced tubes with helical screw-tape of different widths. As shown in the figure, average synergy angle  $\gamma$  between fluid temperature gradient  $\nabla T$  and velocity component gradient  $\nabla u$  has the same trend as PEC shown in the Fig. 8. When the width of the tape is 20 mm, increasing the  $Re$  from 5000 to 6000 seems like leading to a sharp decrement of the angel  $\gamma$ . And as shown in Fig. 8, the PEC values of the tape of 20 mm are higher than the tape of 12.5 mm when the  $Re < 5000$  and are lower than the tape of 17 mm when the  $Re > 6000$ . It is very reasonable for

that because the physical meaning of the angel  $\gamma$  is the same as PEC. Moreover, the decrement of the angel  $\gamma$  and PEC value is very small compared with the values of themselves. Therefore the performance of heat transfer unit will be improved correspondingly.

Fig. 15 shows the variation of average synergy angle  $\theta$  with  $Re$  for heat-transfer enhanced tubes with helical screw-tape of different widths. As shown in the figure, average synergy angle  $\theta$  between fluid velocity  $\mathbf{U}$  and pressure gradient  $\nabla p$  is bigger as the width of helical screw-tape increases, which shows that the direction of velocity  $\mathbf{U}$  deviates more greatly from the direction

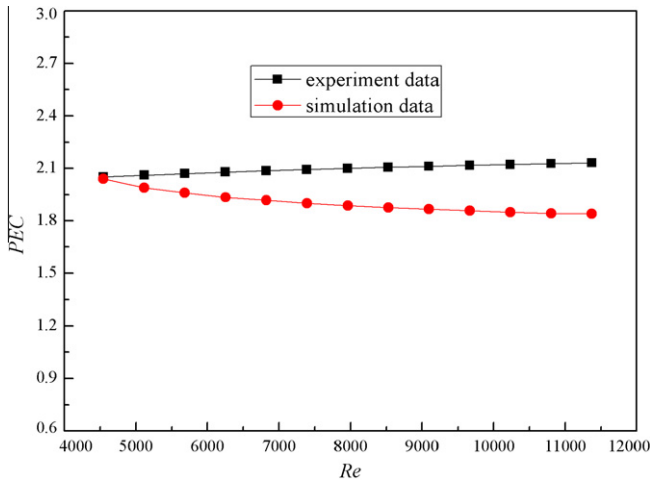


Fig. 11. PEC comparison between experimental data and simulated data.

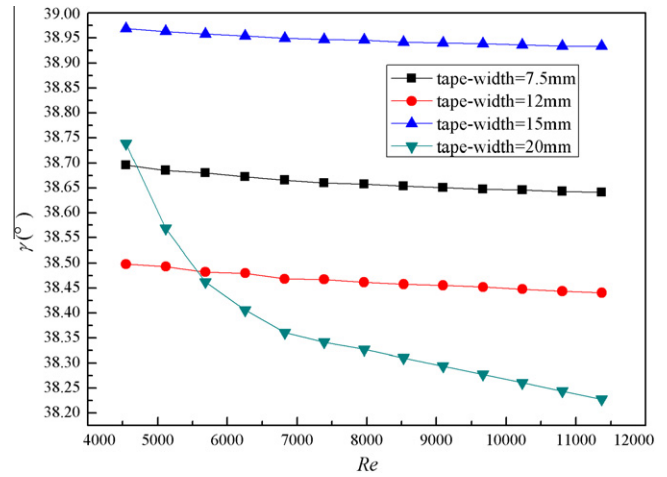


Fig. 14. The variation of average synergy angle  $\gamma$  with  $Re$  for heat-transfer enhanced tubes with helical screw-tape of different widths.

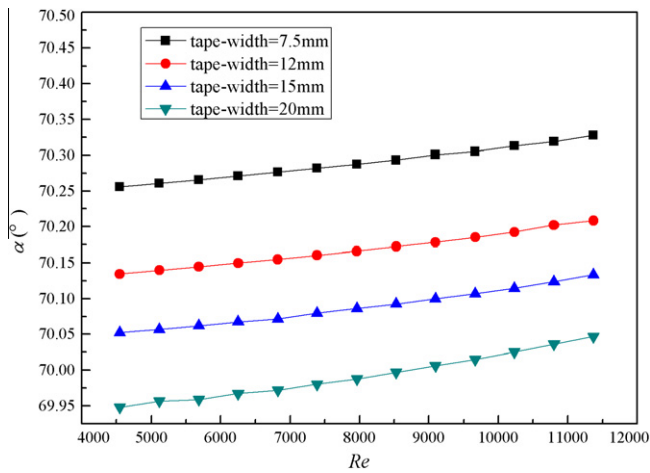


Fig. 12. The variation of average synergy angle  $\alpha$  with  $Re$  for heat-transfer enhanced tubes with helical screw-tape of different widths.

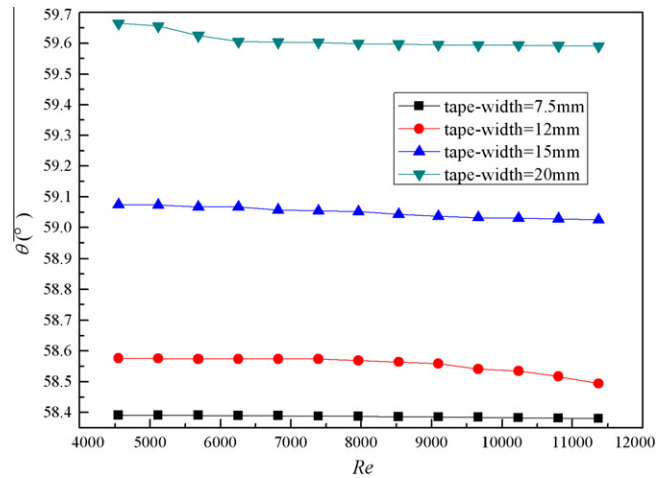


Fig. 15. The variation of average synergy angle  $\theta$  with  $Re$  for heat-transfer enhanced tubes with helical screw-tape of different widths.

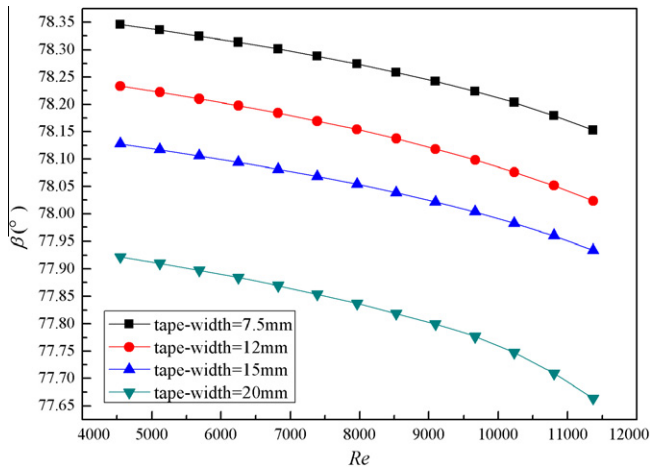


Fig. 13. The variation of average synergy angle  $\beta$  with  $Re$  for heat-transfer enhanced tubes with helical screw-tape of different widths.

Fig. 16 shows the variation of average synergy angle  $\eta$  with  $Re$  for heat-transfer enhanced tubes with helical screw-tape of different widths. As shown in Figs. 16 and 8, it has been found that the variation of average synergy angle  $\eta$  and the PEC value trends are opposite as  $Re$  number and the width of helical screw-tape vary. The average synergy angle  $\eta$  is bigger as the  $Re$  number increases. And the higher the PEC value is, the bigger is the average synergy angle  $\eta$ . Therefore, the smaller the average synergy angle  $\eta$  is, the better is the overall heat transfer performance. In other words, the better coordination between the temperature gradient and pressure gradient, the better the overall heat transfer performance.

### 6. Entropy generation analysis

The present study focuses on steady, turbulent convection in helical screw-tape inserted tubes with uniform wall temperature. The entropy generation analysis is based on the minimal entropy generation principle [24,25]. The analysis is briefly described in the following.

Taking the tape passage of length  $dx$  as the thermodynamic system, the first and second laws can be expressed as

$$mdh = q'dx \tag{28}$$

of pressure gradient  $\nabla p$ , and flow resistance increases more remarkably. Therefore, it is necessary to minimize the synergy between vectors  $\mathbf{U}$  and  $\nabla p$  for designing lower-resistance heat exchangers.

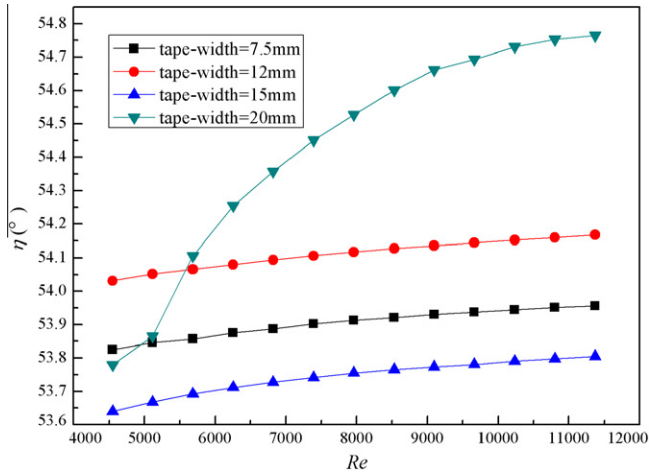


**Fig. 16.** The variation of average synergy angle  $\eta$  with  $Re$  for heat-transfer enhanced tubes with helical screw-tape of different widths.

$$\dot{S}'_{gen} = \dot{m} \frac{ds}{dx} - \frac{q'}{T + \Delta T} \quad (29)$$

where  $\dot{m}$ ,  $q'$ ,  $\dot{S}'_{gen}$  are the mass flow rate in the inserted tubes, the heat transfer rate and the entropy generation rate per unit tape length, respectively. By using the thermodynamic relation

$$Tds = dh - vdp \quad (30)$$

$\dot{S}'_{gen}$  can be written as

$$\dot{S}'_{gen} = \frac{q' \Delta T}{T^2 (1 + \Delta T/T)} + \frac{\dot{m}}{T\rho} \left( -\frac{dP}{dx} \right) \quad (31)$$

Based on Eqs. (17) and (18),  $\dot{S}'_{gen}$  can be expressed by

$$\dot{S}'_{gen} = \frac{(q')^2}{T^2 \pi Nuk + Tq'} + \frac{\dot{m}^3 f}{4T\rho^2 (D/2)^5 \pi^2} \quad (32)$$

The non-dimensional entropy generation number  $N_s$  [24,25] is defined as  $\dot{S}'_{gen}/(q'/T)$  and can be determined from Eq. (32) as

$$N_s = (N_s)_T + (N_s)_P \quad (33)$$

where

$$(N_s)_T = \frac{(q')^2}{T^2 \pi Nuk + Tq'} / (q'/T) \quad (34)$$

$$(N_s)_P = \frac{\dot{m}^3 f}{4T\rho^2 (D/2)^5 \pi^2} / (q'/T) \quad (35)$$

$(N_s)_T$  and  $(N_s)_P$  represent the contributions of entropy generation from heat transfer irreversibility and fluid friction irreversibility, respectively. For describing the contribution of heat transfer entropy generation on overall entropy generation, Paoletti et al. [36] have proposed an irreversibility distribution parameter, Bejan number ( $Be$ ), defined as

$$Be = (N_s)_T / N_s \quad (36)$$

Figs. 17 and 18 show the influences of  $Re$  on  $(N_s)_T$  and  $(N_s)_P$  for heat-transfer enhanced tubes with helical screw-tape of different widths, from which the detail contributions of entropy generation from heat transfer irreversibility and frictional irreversibility can be detected. As  $Re$  number increases,  $(N_s)_T$  decreases and  $(N_s)_P$  increases. The increase of  $Re$  number will enhance the heat transfer performance, which makes the temperature gradient in the flow fields become uniform and, therefore, reduces the heat transfer irreversibility. Meanwhile, the increase of  $Re$  number will cause

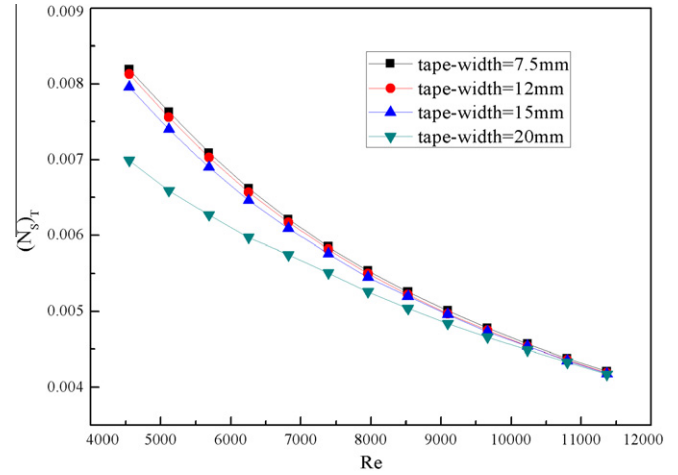


**Fig. 17.** The influence of  $Re$  on  $(N_s)_T$  for heat-transfer enhanced tubes with helical screw-tape of different widths.

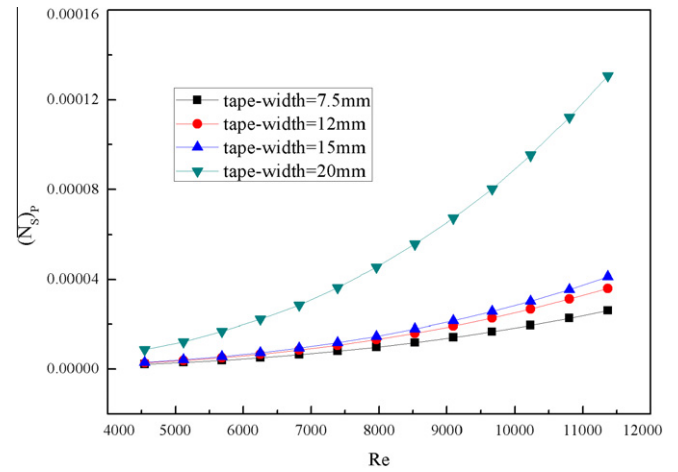


**Fig. 18.** The influence of  $Re$  on  $(N_s)_P$  for heat-transfer enhanced tubes with helical screw-tape of different widths.

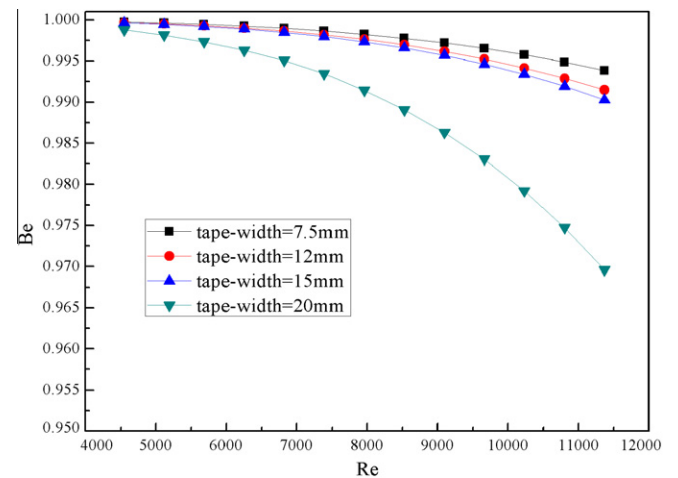


**Fig. 19.** The influence of  $Re$  on  $Be$  for heat-transfer enhanced tubes with helical screw-tape of different widths.

fluid friction to become more serious in the tube and, thus, increase the friction irreversibility. Moreover, as  $Re$  number ranges in



4000 ~ 12000,  $(N_s)_T$  is much larger than  $(N_s)_P$  for all the cases, which implies that the entropy generation is dominated by the heat transfer irreversibility. These results provide worthwhile information for devising a method in a correct direction to reduce irreversibility in flow fields. Fig. 19 shows the influence of  $Re$  on  $Be$  for heat-transfer enhanced tubes with helical screw-tape of different widths. Notably, as  $Re$  increases, the values of  $Be$  decrease monotonically, which implies that the contribution of entropy generation due to fluid friction becomes more important, although the entropy generation is still dominated by the heat transfer irreversibility.

## 7. Conclusion

Heat transfer and friction factor characteristics of a tube fitted with helical screw-tape without core-rod inserts is numerically studied and analyzed by two performance criteria based on the physical quantity synergy principle and minimal entropy generation principle in the present paper. As the  $Re$  number increases, the swirling disturbance generated by helical screw-tape intensifies, thus causing higher temperature and velocity gradient near the tube wall. Therefore both the heat transfer coefficient and the friction factor increase. When the width of helical screw-tape is 15 mm, the fluid flows in core flow area, making the increase of flow resistance in the tube not so obvious and, thereby, the overall performance has improved. And the simulation results show that the physical quantity synergy analysis is in agreement with entropy generation analysis, providing a reliable basis for probing the mechanism of heat transfer enhancement.

## Acknowledgement

This work was supported by the National Key Basic Research Development Program of China (No. 2013CB228302), the National Natural Science Foundation of China (No. 51036003, 51021065) and the Doctor Foundation of Ministry of Education of China (No. 20100142110037).

## References

- [1] A. Bejan, A.D. Kraus, Heat Transfer Handbook, John Wiley, New Jersey, 2003.
- [2] R.M. Manglik, A.E. Bergles, Heat transfer and pressure drop correlations for twisted tape inserts in isothermal tubes. Part II – Transition and turbulent flows, ASME J. Heat Transfer 115 (1993) 890–896.
- [3] R.M. Manglik, A.E. Bergles, Heat transfer and pressure drop correlations for twisted-tape inserts in isothermal tubes. Part I: Laminar flows, Trans. ASME J. Heat Transfer 115 (1993) 881–889.
- [4] S. Eiamsa-ard, P. Promvong, Heat transfer characteristics in a tube fitted with helical screw-tape with and without core-rod inserts, Int. Commun. Heat Mass Transfer 34 (2007) 176–185.
- [5] K. Yang, W. Liu, Forming an equivalent thermal boundary layer for fully-developed laminar tube flow and its field synergy analysis, J. Eng. Thermophys. 28 (2) (2007) 283–285 (in Chinese).
- [6] W. Liu, K. Yang, Mechanism and numerical analysis of heat transfer enhancement in the core flow along a tube, Sci. China Ser. E-Tech 51 (8) (2008) 1195–1202.
- [7] S.K. Saha, U.N. Gaitonde, A.W. Date, Heat transfer and pressure drop characteristics of laminar flow in a circular tube fitted with regularly spaced twisted-tape elements, Exp. Thermal Fluid Sci. 2 (1989) 310–322.
- [8] A.W. Date, U.N. Gaitonde, Development of correlations for predicting characteristics of laminar flow in a tube fitted with regularly spaced twisted-tape elements, Exp. Thermal Fluid Sci. 3 (1990) 373–382.
- [9] Z. Ventsislav, Enhancement of heat transfer by a combination of a single start spirally corrugated tubes with twisted tapes, Exp. Thermal Fluid Sci. 25 (2002) 535–546.
- [10] S.W. Chang, T.L. Yang, J.S. Liou, Heat transfer and pressure drop in tube with broken twisted tape insert, Exp. Thermal Fluid Sci. 32 (2) (2007) 489–501.
- [11] P. Naphon, Heat transfer and pressure drop in the horizontal double pipes with and without twisted tape insert, Int. Commun. Heat Mass Transfer 33 (2006) 166–175.
- [12] P. Sivashanmugam, S. Suresh, Experimental studies on heat transfer and friction factor characteristics of laminar flow through a circular tube fitted with regularly spaced helical screw-tape inserts, Exp. Thermal Fluid Sci. 31 (2007) 301–308.
- [13] P. Sivashanmugam, S. Suresh, Experimental studies on heat transfer and friction factor characteristics of turbulent flow through a circular tube fitted with regularly spaced helical screw-tape inserts, Appl. Thermal Eng. 27 (2007) 1311–1319.
- [14] P. Sivashanmugam, S. Suresh, Experimental studies on heat transfer and friction factor characteristics of laminar flow through a circular tube fitted with helical screw-tape inserts, Appl. Thermal Eng. 26 (2006) 1990–1997.
- [15] P. Sivashanmugam, S. Suresh, Experimental studies on heat transfer and friction factor characteristics of turbulent flow through a circular tube fitted with helical screw-tape inserts, Chem. Eng. Process 46 (2007) 1292–1298.
- [16] S. Eiamsa-ard, P. Promvong, Enhancement of heat transfer in a tube with regularly-spaced helical tape swirl generators, Sol. Energy 78 (2005) 483–494.
- [17] E.Z. Ibrahim, Augmentation of laminar flow and heat transfer in flat tubes by means of helical screw-tape inserts, Energy Convers. Manage. 52 (2011) 250–257.
- [18] J.F. Guo, M.T. Xu, L. Cheng, Numerical investigations of circular tube fitted with helical screw-tape inserts from the viewpoint of field synergy principle, Chem. Eng. Process 49 (2010) 410–417.
- [19] Z.Y. Guo, D.Y. Li, B.X. Wang, A novel concept for convective heat transfer enhancement, Int. J. Heat Mass Transfer 41 (14) (1998) 2221–2225.
- [20] Z.Y. Guo, W.Q. Tao, R.K. Shah, The field synergy (coordination) principle and its applications in enhancing single phase convective heat transfer, Int. J. Heat Mass Transfer 48 (9) (2005) 1797–1807.
- [21] W. Liu, Z.C. Liu, Z.Y. Guo, Physical quantity synergy in laminar flow field of convective heat transfer and analysis of heat transfer enhancement, Chin. Sci. Bull. 54 (19) (2009) 3579–3586.
- [22] W. Liu, Z.C. Liu, S.Y. Huang, Physical quantity synergy in the field of turbulent heat transfer and its analysis for heat transfer enhancement, Chin. Sci. Bull. 55 (23) (2010) 2589–2597.
- [23] W. Liu, Z.C. Liu, T.Z. Ming, Z.Y. Guo, Physical quantity synergy in laminar flow field and its application in heat transfer enhancement, Int. J. Heat Mass Transfer 52 (19–20) (2009) 4669–4672.
- [24] A. Bejan, Entropy Generation Minimization, CRC Press, Boca Raton, FL, 1996.
- [25] A. Bejan, Entropy Generation through Heat and Fluid Flow, Wiley, New York, 1982.
- [26] P.K. Nag, N. Kumar, Second law optimization of convection heat transfer through a duct with constant heat flux, Int. J. Energy Res. 13 (1989) 537–543.
- [27] A.Z. Sahin, Irreversibilities in various duct geometries with constant wall heat flux and laminar flow, Energy 23 (6) (1998) 465–473.
- [28] T.H. Ko, Analysis of optimal Reynolds number for developing laminar forced convection in double sine ducts based on entropy generation minimization principle, Energy Convers. Manage. 47 (2006) 655–670.
- [29] T.H. Ko, Thermodynamic analysis of optimal mass flow rate for fully developed laminar forced convection in a helical coiled tube based on minimal entropy generation principle, Energy Convers. Manage. 47 (2006) 3094–3104.
- [30] Ahmet Tandiroglu, Effect of flow geometry parameters on transient entropy generation for turbulent flow in circular tube with baffle inserts, Energy Convers. Manage. 48 (2007) 898–906.
- [31] E. Ibrahim, M. Moawed, Forced convection and entropy generation from elliptical tubes with longitudinal fins, Energy Convers. Manage. 50 (2009) 1946–1954.
- [32] F.R. Menter, Two-equation eddy-viscosity turbulence models for engineering applications, AIAA J. 32 (1994) 1598–1605.
- [33] R.L. Webb, Performance evaluation criteria for use of enhanced heat transfer surfaces in heat exchanger design, Int. J. Heat Mass Transfer 24 (1981) 715–726.
- [34] J.F. Fan, W.K. Ding, J.F. Zhang, Y.L. He, W.Q. Tao, A performance evaluation plot of enhanced heat transfer techniques, Int. J. Heat Mass Transfer 52 (2009) 33–44.
- [35] S.V. Patankar, Numerical Heat Transfer and Fluid Flow, Hemisphere, Washington, DC, 1980.
- [36] S. Paoletti, F. Rispoli, E. Sciuabba, Calculation of exergetic losses in compact heat exchanger passages, ASME AES 10 (1989) 21–29.